IJASS
International Journal of
Aeronautical and Space Sciences

Check for updates

A Probabilistic Approach for Three-Dimensional Variation Analysis in Aero-engine Rotors Assembly

Siyi Ding[1] · Yuhang He[1] · Xiaohu Zheng[1]

© The Author(s) 2021

Abstract

Rotor assembly is a core tache in the whole process of aero-engine manufacturing. Preventing out-of-tolerance of concentricity is one of the primary tasks. Conventional assembly approaches are based on a manual test with the dial indicator, depending on experience appraises, which lack systematic and quantitative precision design theory. As a result, two issues need to be solved: the modeling problem of complicated geometric variations in three-dimensions, as well as the abnormal distribution of ubiquitous actual deviations. This work attempts to propose a novel probabilistic approach for three-dimensional variation analysis in rotor assembly. Based on rotor's revolving characteristics and multistage stacking process, Jacobian–Torsor model is adopted to establish the variation propagation, and Pearson distribution family is used to derive the probability density function, which can quickly determine the variation distribution pattern and efficiently perform statistical variation analysis. A real case of mechanical assemblies consisting of revolving axisymmetric components is concerned. The results show that the suggested method has a similar accuracy, but much higher efficiency than conventional methods. Calculations agree with the experimentations, and the probability distribution type of the part's variation has an appreciable impact on the final assembly precision.

Keywords Aero-engine rotor · Jacobian–Torsor model · Revolving components assembly · Pearson distribution family · Probability distribution type

1 Introduction

The core of aero-engine consists of a large number of rotor parts. As the high-speed rotating component, aero-engine rotor is usually produced as a combination of different rotor parts, to keep its repairability and maintainability. Due to the presence of part's manufacturing error, datum error, positioning error etc., variation accumulation is inevitable during aero-engine rotor assembly process. Minor variations are caused in the actual component from the nominal geometry [1]. As the assembling process went on, these variations would propagate and drive the final dimensions of assembly out of specification. Reducing product cost and enhancing quality is the tallest target that the enterprise pursues. Statistical variation analysis is an excellent way for predicting

product performance in the initial design stage [2]. It is actually a quantitative design method which can analyze the size effect containing various tolerance specification quantitatively, to meet both design and manufacturing requirements.

Machinery quality is affected by many factors during processing, such as tool wearing, clamping way, human factors, etc. When various influencing factors are generated randomly, parts manufacturing variations are in accordance with normal distribution. Normality assumption is convenient for statistical evaluation due to its symmetry, and beneficial to theoretical study. On this account, traditional methods of tolerance design and variation analysis have widely adopted the hypothesis that the random variables of parts variations are normally distributed. Conventional methods for exploring assembly variation propagation are mainly based on a manual test with the dial indicator, depending on experience appraises, or extremum method [3–6], or the mean square root (MSR) method [7–9], which lack of systematic and quantitative precision design theory. However, the result calculated by extremum method is far too restrictive that would lead to high production cost, while the MSR

✉ Siyi Ding
dingsiy@dhu.edu.cn

1   Present Address: Institute of Artificial Intelligence,
    Dong Hua University, 2999 North Renmin Road,
    Shanghai 201600, China

method concerns mean-square variation that is primarily suitable for solving the plane size-chain problem [10–12]. These methods are used frequently in the case of normal distribution. Meanwhile, they are underdeveloped in regard to the geometrical errors in the spatial 3D state [7, 13].

However, in practical matters, most variation distribution of part variable disobey the normal type. For example, if tool wear plays the dominant role during processing, the actual variable variation of part's dimension would follow uniform distribution (flat-topped distribution); if a manufacturing process involves the simultaneous processing of two machine tools, the mixing variable variations of the parts would satisfy bimodal distribution; when adopting a trial cutting approach to fabricate shaft journals or apertures, operators tend to keep a certain machining allowance deliberately, which would cause skewed distribution of the final dimensional variables. The most versatile and popular way for statistical variation analysis is Monte Carlo (MC) simulation, which is a numerical method and suitable for data abnormal distribution. According to known or assumed statistical distributions, random variation of each component can be generated, and the corresponding critical feature will be calculated for each set of part variables. By this means, the probability can be worked out indicating that whether the key characteristic is satisfied or not. Nowadays, MC simulation method has been developed into the core of most of the commercial software for 3D tolerance analysis, such as 3DCS, VSA, CATS-1DXL and CETOL, to name a few. However, to realize accurate prediction, a large number of data samples are desired [14–17], inevitably causing the time-consuming calculation, which is the obvious drawback to MC approach. This problem becomes more prominent when variation analysis is performed within an iterative loop of a more complicated variation propagation issue, and the solution would be extremely computationally expensive.

From the above, it is observed that the statistical methods developed so far are not very effective for solving the issue of 3D variation propagation with abnormal distribution. As this paper focuses on the general case of the mechanical assembly consisting of revolving axisymmetric components [18–23], which is widely used in the aero-engine industry, especially in the engine rotors fabricating [24, 25], there is a clear need to adopt a simple and rapid probabilistic approach for determining the likelihood that the mechanical assembly is acceptable or not, so as to consider the practical distribution of variation variables and efficiently deal with large sets of data.

Recently, Yang et al. [26] researched the density distribution of rotation error in aero-engine assembly. Probability density functions (PDF) for the eccentricity were formulized based on the assumption that the component variations were statistically independent, zero-mean Gaussian random variables with known standard deviations. This PDF was essentially a Rayleigh distribution and results were calculated more efficiently than Monte Carlo simulations. Ghie [27] enriched the Jacobian–Torsor model combining with uncertain measurements. The uncertainty magnitudes were estimated using the approximate normal distribution method and spread to FR by linear superposition. However, this PDF could not give consideration to the skewed distribution of variables. Ahsanullah and Hamedani [28], on the basis of the conditional distribution of generalized order statistics, tried to study more detail on the various characterizations of certain univariate continuous distributions. It provided a base of further research of multivariable continuous distributions, which was applicable to the stream of multisource variation modelling. Kharoufehy and Chandraz [29] used a discretized, multivariate kernel density estimate and a simple transformation to approximate the probability distribution of the overall assembly characteristic. By this method, the typical assumptions of independence and normality could possibly be relaxed when the number of components being combined was small. But it was hard to select the smoothing parameter (h), which would yield possibly dramatically different distributions. From this review, we can know that modelling PDF is very complex and it is difficult to consider the polymorphic probability density distribution. In this paper, we will introduce an innovation of Pearson distribution family [30, 31] to address this issue, which will be discussed detailedly in Sect. 2.2.

In addition, variation accumulation of the rotor assembling process can be hardly described by reason of the uncertainty inherent in a complex assembly. In the past few years, three-dimensional variation modelling methods have been studied. Four mainstream modelling approaches among them have been reported largely and studied deeply, i.e., the direct linearization method (DLM), the tolerance map (T-Map) model, the matrix model and the unified Jacobian–Torsor (J–T) model. The DLM [32, 33] uses vectors to represent either component dimensions or assembly dimensions. Although all types of tolerances can be modeled, it is difficult to define the joint types and the effects of geometric variations, as well as the interaction between geometric tolerance and dimensional tolerance is indistinct. The T-Map model [34, 35] is a hypothetical Euclidean volume that is fully consistent with the ASME standard, but the Minkowski operation of T-Map for tolerance propagation and the visualization of higher-dimensional maps are not straightforward. The matrix model [36, 37] uses a displacement matrix to describe small displacements of a feature within its tolerance zone. Although it is suitable for tolerance propagation analysis, the computation process is very difficult and time-consuming, under the action of large numbers of constraint inequalities, especially non-linear inequalities. The J–T theory [38, 39] is well suited to a complex assembly that contains large numbers of joints and geometric tolerances.

It combines the advantages of the torsor model which is suitable for variation representation and the Jacobian matrix which is suitable for variation propagation. Therefore, the J–T model is well suited to a complex assembly that contains large numbers of joints and geometric deviations. Parts of aero-engine rotors are usually rich in variation information and joints of cylindrical and planar surfaces. In view of the rotor's configuration and assembling characteristics of aero-engine, the J–T model is used to build the variation propagation model of multi-stage stackup in this paper.

Therefore, based on the above aspects, this paper will propose a novel probabilistic analysis method combined with Jacobian–Torsor modelling theory, to take account of random component variability during revolving components assembly. The rest of the paper is organized as follows. Section 2 reminds the theory of the unified Jacobian–Torsor and Pearson distribution family. Section 3 explores the statistical analysis method and gives the specific solution. Section 4 proves this method by a realistic case originating in aero-engine subassembly. Section 5 discusses the results and Sect. 6 is conclusions.

2 Related Works

2.1 Description of Jacobian–Torsor Model

The traditional J–T model consists of the Jacobian matrix and torsor model. The Jacobian matrix originates from the expression in robot kinematics, which is:

$$[J]_{\text{FE}i} = \begin{bmatrix} [R_0^i]_{3\times3} \cdot [R_{\text{Pt}i}]_{3\times3} & \vdots & [W_i^n]_{3\times3} \cdot \left([R_0^i]_{3\times3} \cdot [R_{\text{Pt}i}]_{3\times3} \right) \\ \cdots & \vdots & \cdots \\ [0]_{3\times3} & \vdots & [R_0^i]_{3\times3} \cdot [R_{\text{Pt}i}]_{3\times3} \end{bmatrix},$$

(1)

where $[R_0^i]$ represents the ith frame orientation; $[R_{\text{Pt}i}]$ is a projection matrix that allows efficient transformation of variation direction to the target analysis direction; $[W_i^n]$ describes the positional relation between adjacent frames in the form of skew-symmetric matrix. It is defined as Eq. (2):

$$[W_i^n]_{3\times3} = \begin{bmatrix} 0 & \mathrm{d}z_i^n & -\mathrm{d}y_i^n \\ -\mathrm{d}z_i^n & 0 & \mathrm{d}x_i^n \\ \mathrm{d}y_i^n & -\mathrm{d}x_i^n & 0 \end{bmatrix}.$$

(2)

The subscript FE_i in $[J]$ means the ith functional element. Two categories of FEs exist in the assembly: internal FE (IFE) and contact FE (CFE). The former denotes two mating features on the same part and the latter denotes two mating features on separated ones. FEs' Variations could be delivered to the FR (functional requirement) by Jacobian matrix. It is observed that the Jacobian model only expresses the three-dimensional geometric relationship between the

features, without defining the objects and contents propagated, so it is an incomplete model.

Torsor model can describe the ideal position and orientation of any surfaces by three translational vectors and three rotational vectors. Figure 1 shows a torsor model to express the position and orientation of an ideal surface. Assuming t is the tolerance between arbitrary feature S_1 and nominal feature S_0, there is:

$$T_{1-0} = \begin{bmatrix} u & v & w & \alpha & \beta & \gamma \end{bmatrix}^T,$$

(3)

where u, v, w denote translation vectors along x, y and z axes; α, β and γ denote rotation vectors around x, y and z axes respectively in local coordinate system.

Hervé [40] presented the displacements set theory, defining the non-invariant degrees, which determined the effective vectors. According to this, some vectors could be taken zero value to simplify the modeling process. Table 1 has shown seven primary torsor forms.

It is observed that the torsor model fully expresses the position and direction of the feature in 3D space. If combining with the tolerance constraint equation, a complete syntactic and semantic representations of geometric tolerances can be construed. But it is also observed that the torsor model is unable to characterize the variation propagation. It will probably have to be with the help of some transfer function or transfer matrix.

The variation of torsors propagates to the target characteristics taking advantage of Jacobian matrix, which accurately expresses the relative positions and orientations between the local and global coordinates. The unified J–T model takes synthesize advantages of the Jacobian matrix and torsor model. The former is appropriate for variation propagation and the latter is suited to variation expression [41, 42]. The form of J–T model could be written as:
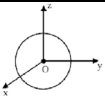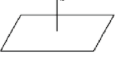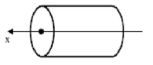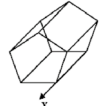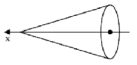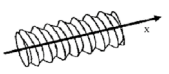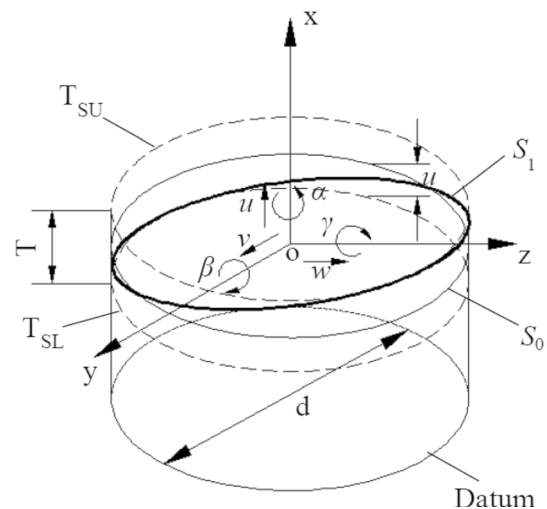

Fig. 1 Torsor model in its tolerance zone

Table 1 Features and their Torsor models

No.	Element	Type of feature	Torsor model
1	Sphere		$\begin{Bmatrix} - & u \\ - & v \\ - & w \end{Bmatrix}$
2	Plane		$\begin{Bmatrix} - & u \\ \beta & - \\ \gamma & - \end{Bmatrix}$
3	Cylindrical surface		$\begin{Bmatrix} - & - \\ \beta & v \\ \gamma & w \end{Bmatrix}$
4	Prismatic surface		$\begin{Bmatrix} \alpha & - \\ \beta & v \\ \gamma & w \end{Bmatrix}$
5	Revolution surface		$\begin{Bmatrix} - & u \\ \beta & v \\ \gamma & w \end{Bmatrix}$
6	Helicoid		$\begin{Bmatrix} - & u \\ \beta & v \\ \gamma & w \end{Bmatrix} \Leftrightarrow u \neq \dfrac{pa}{2\pi}$
7	Arbitrary shape curved surface		$\begin{Bmatrix} \alpha & u \\ \beta & v \\ \gamma & w \end{Bmatrix}$

where "–" means the vector is invalid in the corresponding direction. a and p, respectively, denote thread tooth link angle and screw pitch.

$$\begin{bmatrix} (\underline{u},\overline{u}) \\ (\underline{v},\overline{v}) \\ (\underline{w},\overline{w}) \\ (\underline{\alpha},\overline{\alpha}) \\ (\underline{\beta},\overline{\beta}) \\ (\underline{\gamma},\overline{\gamma}) \end{bmatrix}_{\mathrm{FR}} = \begin{bmatrix} [J]_{\mathrm{FE1}} & \cdots & [J]_{\mathrm{FE}n} \end{bmatrix} \times \begin{bmatrix} \begin{bmatrix} (\underline{u},\overline{u}) \\ (\underline{v},\overline{v}) \\ (\underline{w},\overline{w}) \\ (\underline{\alpha},\overline{\alpha}) \\ (\underline{\beta},\overline{\beta}) \\ (\underline{\gamma},\overline{\gamma}) \end{bmatrix}_{\mathrm{FE1}} \cdots \begin{bmatrix} (\underline{u},\overline{u}) \\ (\underline{v},\overline{v}) \\ (\underline{w},\overline{w}) \\ (\underline{\alpha},\overline{\alpha}) \\ (\underline{\beta},\overline{\beta}) \\ (\underline{\gamma},\overline{\gamma}) \end{bmatrix}_{\mathrm{FE}n} \end{bmatrix}^{T},$$

(4)

where $(\underline{\alpha},\overline{\alpha})$ is the variation zone, and β, γ, u, v and w follow the similar way as α. Other parameters have the same meanings as those in Eq. (1).

2.2 Pearson Distribution Family

Statistician K. Pearson [30, 31] firstly proposed the Pearson system of distributions in 1895, which involved the normal distribution and diversified abnormal distributions. The Pearson system included four main types of parameters, which were used to reflect the general distribution in practice. Its probability density function (PDF) $f(x)$ was determined by the differential equation as follows:

$$\frac{\mathrm{d}f(x)}{\mathrm{d}x} = \frac{(a_0 + a_1 x)f(x)}{b_0 + b_1 x + b_2 x^2}.$$

(5)

When $a_1 = 1$, the parameters a_0, b_0, b_1 and b_2 entirely depend on the first four orders of the central moments of the distribution parameters μ_1, μ_2, μ_3, and μ_4. It also could be indicated as the moment ratios as $\beta_1 = \mu_3^2/\mu_2^3$ and $\beta_2 = \mu_4/\mu_2^2$, which are shown as follows:

$$a_0 = -b_1,$$

(6)

$$b_0 = A\sigma^2(4\sigma^2\mu_4 - 3\mu_3^2) = B\sigma^2(4\beta_2 - 3\beta_1),$$

(7)

$$b_1 = A\mu_3(\mu_4 + 3\sigma^4) = B\sigma\sqrt{\beta_1}(\beta_2 + 3),$$

(8)

$$b_2 = A(2\sigma^2\mu_4 - 3\mu_3^2 - 6\sigma^6) = B(2\beta_2 - 3\beta_1 - 6),$$

(9)

where

$$A = -(10\sigma^2\mu_4 - 18\sigma^6 - 12\mu_3^2)^{-1},$$

(10)

$$B = -(10\beta_2 - 12\beta_1 - 18)^{-1}.$$

(11)

The general solution of $f(x)$ is:

$$f(x) = C\exp\left\{-\int \frac{a_0 + a_1 x}{b_0 + b_1 x + b_2 x^2}\mathrm{d}x\right\}.$$

(12)

Based on the above analysis, Pearson system will be elaborated as seven distribution patterns [43, 44], which are:

Distribution pattern I: $f(x) = \dfrac{(p + x)^{\alpha-1}(q - x)^{\beta-1}}{B(\alpha, \beta)(p + q)^{\alpha+\beta-1}}, (-p < x < q),$

(13)

where p, q and α, β are all greater than zero, and $\alpha/p = \beta/q$. It is essentially Beta distribution.

Distribution pattern II: $f(x) = \dfrac{(p^2 - x^2)^{\alpha-1}}{B(\alpha, \alpha)(2p)^{2\alpha-1}}, (-p < x < p),$

(14)

where $p, \alpha > 0$. It is a special case of pattern I where $p = q, \alpha = \beta$, and the distribution curve of pattern II is a symmetrical U type curve.

Distribution pattern III : $f(x)$
$$= \frac{\lambda^\alpha}{\Gamma(\alpha)}(x - \mu)^{\alpha-1}e^{-\lambda(x-\mu)}, (\mu < x < \infty),$$

(15)

where $\mu, \alpha, \lambda > 0$. It is a shifted gamma distribution where μ is a location parameter.

Distribution pattern IV : $f(x) = \dfrac{\exp\left(-\lambda\arctan\frac{x}{\beta}\right)}{I(\alpha, \beta, \lambda)(\beta^2 + x^2)^\alpha},$

(16)

where $\alpha \geq 1/2, \lambda > 0, \beta > 0, I(\alpha, \beta, \lambda) = \int_{-\infty}^{\infty} \frac{\exp\left(-\lambda\arctan\frac{x}{\beta}\right)}{(\beta^2+x^2)^\alpha}\mathrm{d}x.$

Distribution pattern V : $f(x)$
$$= \frac{\lambda^\alpha}{\Gamma(\alpha)}(x - \mu)^{-(\alpha+1)}e^{-\lambda(x-\mu)^{-1}}, (\mu < x < \infty),$$

(17)

where $\alpha, \lambda > 0$. It is a shifted inverse gamma distribution where μ is a location parameter.

Distribution pattern VI : $f(x)$

$$= \frac{(x+p)^{-(\alpha+\beta)}(x-q)^{\alpha-1}}{B(\alpha,\beta)(p+q)^\beta}, (q < x < \infty), \tag{18}$$

w h e r e $\alpha, \beta > 0$.   W h i l e $p = 1, q = 0$,
$f(x) = \frac{1}{B(\alpha,\beta)}(x+1)^{-(\alpha+\beta)}x^{\alpha-1}, (0 < x < \infty)$.

Distribution pattern VII : $f(x) = \dfrac{p(p^2+x^2)^{-\alpha}}{B\left(\alpha - \frac{1}{2}, \frac{1}{2}\right)}, \tag{19}$

where $\alpha \geq 1/2, p > 0$. Student's *t*-distribution belongs to this kind of distribution.

Besides these seven main types of distribution, Pearson distribution family also includes some special cases, such as normal distribution, power function distribution, exponential distribution, etc. Seven types of Pearson distribution can be identified according to the different distributions of the quadratic equation roots of $b_0 + b_1 x + b_2 x^2 = 0$. Assuming $D = b_1^2 - 4b_0 b_2, \lambda = b_1^2 \div (4b_0 b_2)$, the Pearson distribution pattern could be distinguished by the value of D and λ, as demonstrated in Table 2.

It can be also categorized in terms of moment ratios β_1, β_2. The λ in first approach of classification can be represented as $\lambda = \frac{1}{4}\beta_1 (\beta_2 + 3)^2 (4\beta_2 - 3\beta_1)^{-1} (2\beta_2 - 3\beta_1 - 6)^{-1}$. The details are shown in Table 3.

3 Statistical Algorithm

In this paper, simplified cylindrical components were used to illustrate the assembling process, where coordinate system 0 represented the global coordinate system and the revolving axis was denoted with a virtual centerline that passed through the bottom part's base centre and was perpendicular to its datum plane, as illustrated in Fig. 2.

Before applying the model, it should be noted that for every rotor part, two assumptions will be made to simplify operations.

- As the Jacobian matrix cannot solve the structure of partial parallel connection well, the locating spigot round (A) contact pair of the cylindrical joint) is ignored, and the flange plane (B) contact pair of the planar joint) of the rotor part is reserved. Generally, the contact pair of B shows the most significant effect due to that the mounting edge of area B is much larger than that of A. Figure 3a has illustrated this difference.
- This paper adopts a unified solution that each rotor's bottom face is set as the datum, while the top face is designated by a geometric tolerance with the corresponding

Table 2 Method 1 to determine Pearson distribution types

a_1	D	λ	Distribution pattern	Remarks
0	0	0	Exponential distribution	
$\neq 0$	> 0	$-\infty$	Pattern VII	$b_0 = 0$
		$(-\infty, 0)$	Pattern I	
		0	Pattern II	
		$(1, \infty)$	Pattern VI	
		∞	Pattern III	
	$= 0$	1	Pattern V	$b_1 = b_2 = 0$
		Uncertain	Normal distribution	
	< 0	$(0, 1)$	Pattern IV	

datum plane. Figure 3b has illustrated the standardized rotor part to simplify and maintain the geometric tolerance information.

On the basis of the above assumptions, variations propagate from rotor's bottom to the top. According to the characteristics of Jacobian matrix, $[[\boldsymbol{J}_1, \boldsymbol{J}_2, \boldsymbol{J}_3, \boldsymbol{J}_4, \boldsymbol{J}_5, \boldsymbol{J}_6]_{FE1}, [\boldsymbol{J}_1, \boldsymbol{J}_2, \boldsymbol{J}_3, \boldsymbol{J}_4, \boldsymbol{J}_5, \boldsymbol{J}_6]_{FE2}, \ldots, [\boldsymbol{J}_1, \boldsymbol{J}_2, \boldsymbol{J}_3, \boldsymbol{J}_4, \boldsymbol{J}_5, \boldsymbol{J}_6]_{FEn}]$ represents the transfer process of the variations from FE_1 to FE_n. Therefore, Eq. (4) using interval-based uncertainty zone representation can be further rewritten as Eq. (20), which is fit for deterministic variation analysis and beneficial to the error compensation.

$$\begin{bmatrix} u_m \\ v_m \\ w_m \\ \alpha_m \\ \beta_m \\ \gamma_m \end{bmatrix}_{FR} = \begin{bmatrix} [J]_{FE1} & \cdots & [J]_{FEn} \end{bmatrix} \times \begin{bmatrix} \begin{bmatrix} u_1 \\ v_1 \\ w_1 \\ \alpha_1 \\ \beta_1 \\ \gamma_1 \end{bmatrix}_{FE1} & \cdots & \begin{bmatrix} u_n \\ v_n \\ w_n \\ \alpha_n \\ \beta_n \\ \gamma_n \end{bmatrix}_{FEn} \end{bmatrix}^T. \tag{20}$$

Equation (20) could be characterized as $y_{FR} = f (u_i, v_i, w_i, \alpha_i, \beta_i, \gamma_i), (i = 1, 2, \ldots, n)$, where y_{FR} denotes the variation of FR, and $(u_i, v_i, w_i, \alpha_i, \beta_i, \gamma_i)$ represents the translation variation or rotation variation of FE in different direction. Assuming that all the variation of FE is independent of each another and distributed randomly, we could calculate the four main parameters of FR in virtue of the parameters of FE. Based on the characteristics of Pearson system, the distribution pattern could be deduced and the PDF could be determined when the first four central moments are derived. As for arbitrary distribution, the μ_1 which is the first-order central moment will be equal to zero identically; the μ_2 which is the second-order central moment represents data dispersion degree, equaling to the variance σ^2; the μ_3 which is the third-order central moment is related to S (coefficient of skewness), and $S = \mu_3/\sigma^3$; and the μ_4 which is related to K (coefficient of

Table 3 Method 2 to determine Pearson distribution types

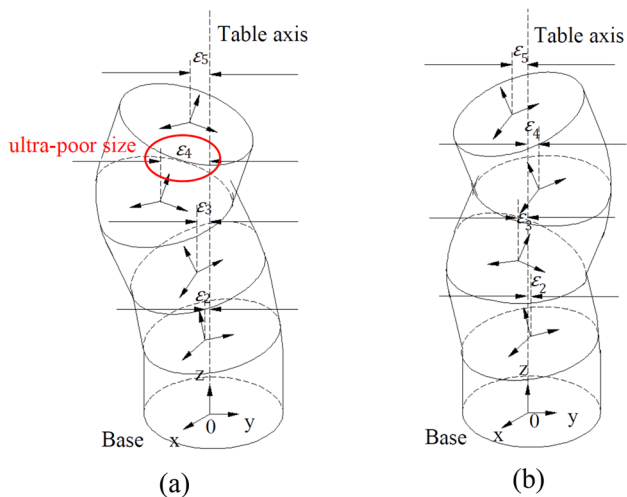|	Pattern I	Pattern II	Pattern III	Pattern IV	Pattern V	Pattern VI	Pattern VII
	$\lambda < 0$	$\beta_1 = 0$ $\beta_2 < 3$	$2\beta_2 - 3\beta_1$ $-6 = 0$	$0 < \lambda < 1$	$\lambda = 1$	$\lambda > 1$	$\beta_1 = 0$ $\beta_2 > 3$

Fig. 2 Assembly accuracy prediction: **a** poor assembly and **b** qualified assembly

kurtosis) is formulated as $K = \mu_4/\sigma^4$. Due to the four main parameters (mean value, variance, skewness and kurtosis) of an arbitrary probability distribution could characterize the distribution shape visually, we will calculate the four main parameters to obtain the first four central moments indirectly in this article. Computational formulas of the mean value, variance, skewness and kurtosis can be consulted in reference [45].
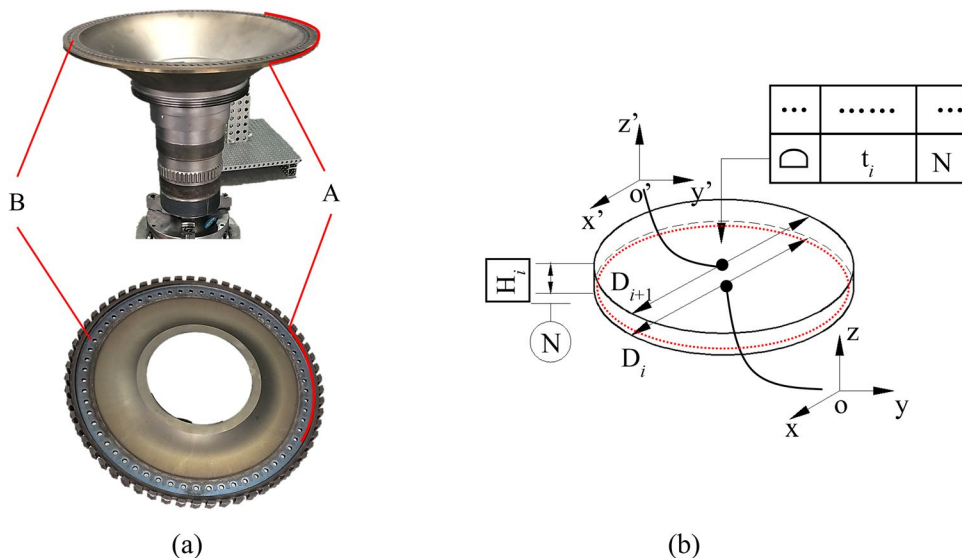
Back in Eq. (20), hence a_0, b_0, b_1 and b_2 could be gained with the known distribution parameter of FR. Distribution pattern would be determined by adopting the method of Pearson distribution family (Tables 2 or 3) and the PDF could be expressed. Ultimately the probability distribution curve could be derived and the assembly qualified rate could be worked out. The solution procedure is shown in Fig. 4.

4 Case Study

To prove the feasibility of the new method mentioned above, a real rotor assembly originating in an aero-engine will be used for statistical variation analyzing. As shown in Fig. 5, the aero-engine rotor assembly consists of four revolving components with high precision and all relevant coordinates have been established. Frame 0 is the overall coordination system and the revolving axis is specified as the center line that passes through the datum plane of the bottom part and is perpendicular to it.

Every part's dimension and composite tolerance have been shown in Table 4, which have been illustrated in Fig. 5. The pose position and orientation of the whole assembly are directly affected by each rotor's geometric variations and their joints. Various errors accumulate on the final rotor part, which are very important for performance stability of aero-engine assembly. To meet the technical requirement, concentricity control of rotor assembly is very critical. On

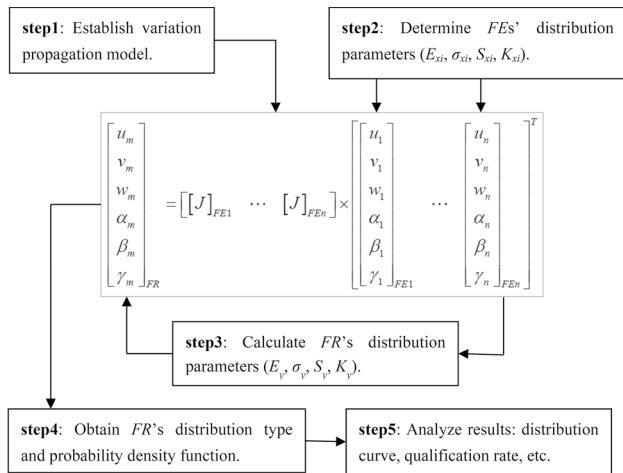**Fig. 3** The rotor parts: **a** the actual parts and **b** the geometric model

$$\begin{bmatrix} u_m \\ v_m \\ w_m \\ \alpha_m \\ \beta_m \\ \gamma_m \end{bmatrix}_{FR} = \begin{bmatrix} [J]_{FE1} & \cdots & [J]_{FEn} \end{bmatrix} \times \left(\begin{bmatrix} u_1 \\ v_1 \\ w_1 \\ \alpha_1 \\ \beta_1 \\ \gamma_1 \end{bmatrix}_{FE1} \cdots \begin{bmatrix} u_n \\ v_n \\ w_n \\ \alpha_n \\ \beta_n \\ \gamma_n \end{bmatrix}_{FEn} \right)^T$$

step1: Establish variation propagation model.

step2: Determine FEs' distribution parameters $(E_{xi}, \sigma_{xi}, S_{xi}, K_{xi})$.

step3: Calculate FR's distribution parameters $(E_y, \sigma_y, S_y, K_y)$.

step4: Obtain FR's distribution type and probability density function.

step5: Analyze results: distribution curve, qualification rate, etc.

Fig. 4 Statistical variation analysis using Pearson distribution family

the basis of statistical variation analysis approach that is referred in Sect. 3, the specific calculation process is demonstrated as follows.

First, a coordinate reference system and the assembly relation graph were built. The global reference system 0 was established in the center of the rotor base, and local coordinate systems were set in the center of related adjacent surfaces. The assembly relation graph was illustrated in Fig. 6. FR was the pose accuracy of the top part in regard to the coordinate system 0. It was observed that there was a serial path for variation propagation from FEi to FR, i.e. IFE_1-CFE_1-IFE_2-CFE_2-IFE_3-CFE_3-IFE_4-FR.

Secondly, according to the connection graph mentioned above, the variation propagation model would be established. Based on the expression of the unified Jacobian–Torsor model, the Jacobian matrix and the tolerancing torsor of FEi could be

calculated, as well as its corresponding variation range could be determined. Table 5 has shown the detailed expression forms.

Next, according to Eq. (20), by multiplying the Jacobian matrixes and torsors together, the expression of the results could be derived as Eq. (21). In this case, the components' eccentricity along one certain direction was arbitrarily chosen for demonstration. For example, in the direction of x axis, the cumulative variation could be extracted from u_4 in Eq. (21) and formulized as Eq. (22). And it was also important to note that all the effective vectors in tolerancing torsors should satisfy the variation requirement, as listed in the third column of Table 5.

$$[FR]_4 = \begin{bmatrix} u_4 \\ v_4 \\ w_4 \\ \alpha_4 \\ \beta_4 \\ \gamma_4 \end{bmatrix} = \begin{bmatrix} \sum_{i=1}^{4}\left[\beta_i \times \left(\sum_{j=1}^{i} H_j\right)\right] \\ \sum_{i=1}^{4}\left[-\alpha_i \times \left(\sum_{j=1}^{i} H_j\right)\right] \\ \sum_{i=1}^{4} w_i \\ \sum_{i=1}^{4} \alpha_i \\ \sum_{i=1}^{4} \beta_i \\ 0 \end{bmatrix}$$

$$= \begin{bmatrix} 0.02\beta_1 + 0.04\beta_2 + 0.06\beta_3 + 0.08\beta_4 \\ -0.02\alpha_1 - 0.04\alpha_2 - 0.06\alpha_3 - 0.08\alpha_4 \\ w_1 + w_2 + w_3 + w_4 \\ \alpha_1 + \alpha_2 + \alpha_3 + \alpha_4 \\ \beta_1 + \beta_2 + \beta_3 + \beta_4 \\ 0 \end{bmatrix},$$

(21)

$$y_{u_4} = 0.02\beta_1 + 0.04\beta_2 + 0.06\beta_3 + 0.08\beta_4.$$ (22)
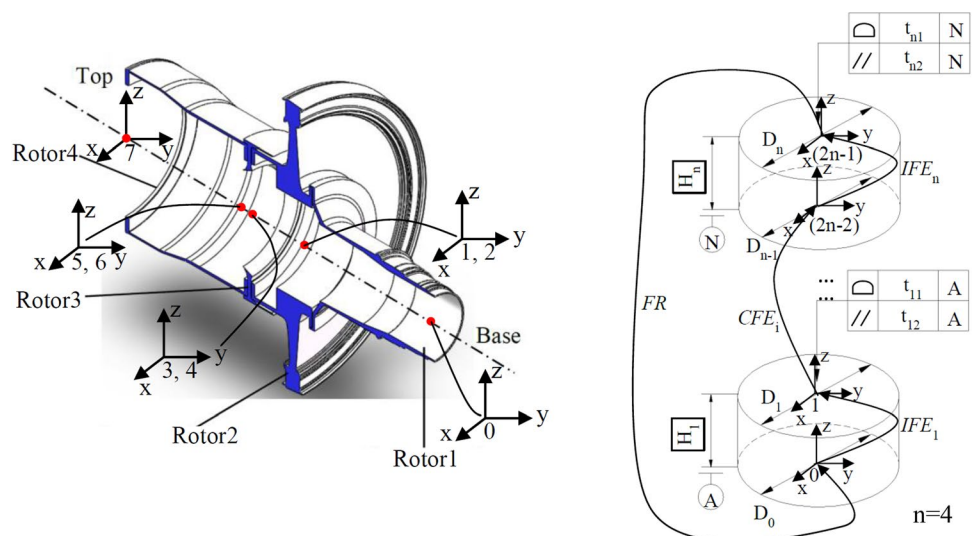
Fig. 5 Four-stage rotor assembly

Table 4 Dimensions and geometric tolerances of each component

Component	Base diameter (mm)	Top diameter (mm)	Height (mm)	Profile tolerance (mm)	Parallelism tolerance (mm)
1	107	405	315	0.020	0.015
2	405	410	135	0.020	0.015
3	410	400	165	0.020	0.015
4	400	440	365	0.020	0.015

Thirdly, calculate the distribution parameters of FEs and FR, on the basis of Eqs. (23) ∼ (26) below. Then the FR's distribution type could be determined and its PDF would be deduced.

$$E_y = \sum_{i=1}^{n} a_i E_{x_i}, \tag{23}$$

$$\sigma_y^2 = \sum_{i=1}^{n} a_i^2 \sigma_{x_i}^2, \tag{24}$$

$$S_y = \frac{E[y - E(y)]^3}{\sigma_y^3} = \frac{\sum_{i=1}^{n} a_i^3 S_{x_i} \sigma_{x_i}^3}{\sigma_y^3}, \tag{25}$$

$$K_y = \frac{E[y - E(y)]^4}{\sigma_y^4} = \left(\sum_{i=1}^{n} a_i^4 K_{x_i} \sigma_{x_i}^4 + 6 \sum_{i=1}^{n-1} \sum_{j=i+1}^{n} a_i^2 a_j^2 \sigma_{x_i}^2 \sigma_{x_j}^2 \right) / \sigma_y^4, \tag{26}$$

where a_i represented the sensitivity coefficient, E_{xi} and E_y respectively were the mathematical expectations of the ith FE and FR. The σ_{xi} and σ_y, respectively, were the standard deviations of the ith FE and FR. The S_{xi} and S_y denoted skewness coefficient of the ith FE and FR. The K_{xi} and K_y denoted the kurtosis coefficient of the ith FE and FR.

It should be noted that in abnormal distribution models, Beta distribution can handle various laws of the probability of manufacturing variations [8]. There are four parameters

Fig. 6 Connection graph of four-stage assembly

in the Beta distribution function, which are two location parameters and two shape parameters. According to different parameter values, it can characterize many different distribution patterns, such as Rayleigh distribution, uniform distribution, trapezium distribution, triangular distribution, etc. As a result, in this paper we would use Beta distribution to simulate skewed distribution of the actual manufacturing practice.

The most common types of probability distribution in the machining process mainly consist of normal distribution, skewed distribution, uniform distribution (flat-topped distribution), etc. [46]. To test the influence of variation distribution type on the final assembly precision, the distribution type of FE was supposed to follow the above distribution patterns, respectively. In the following, four probability combinations would be researched as listed in Table 6, where the skewed distribution would be simulated by Beta distribution approximation.

The distribution parameters of *FR* could be calculated based on Eqs. (23) to (26). The distribution results were shown in Table 7. According to Eqs. (6) to (11), the values of a_0, b_0, b_1, b_2 could be further derived. Then referring to Tables 2 and 3, the variation distribution pattern of FR could be determined. The results had been listed in the last column of Table 7.

In the end, the PDF would be solved by adopting Pearson distribution family formulas of pattern IV and VI. By using Matlab function ([p, type, coefs] = pearspdf (X, mu, sigma, skew, kurt)), the probability density of Pearson distribution with mean 'mu', standard deviation 'sigma', skewness 'skew' and kurtosis 'kurt' could be easily worked out, which was evaluated at the value of X.

The qualification rates of four combinations were calculated and compared with the results of MC simulation, which have been shown in Table 8. It should be noted that in this case, the simulated number of MC was set to 10,000, which was beneficial to balance accuracy with efficiency. Meanwhile with regard to the qualification rate, in accordance with engineering requirements, FR should fall in the qualified range of 0.038 mm. See the table below for more details.
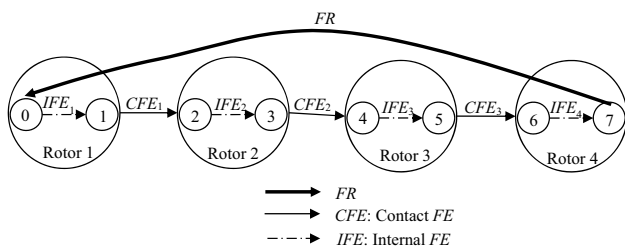
Table 5 Jacobian matrixes and tolerancing torsors

No	FE_s	Jacobian matrixes	Tolerancing torsors	Variations
1	IFE_1	$\begin{bmatrix} 1 & 0 & 0 & 0 & 315 & 0 \\ 0 & 1 & 0 & -315 & 0 & 0 \\ 0 & 0 & 1 & 0 & 0 & 0 \\ 0 & 0 & 0 & 1 & 0 & 0 \\ 0 & 0 & 0 & 0 & 1 & 0 \\ 0 & 0 & 0 & 0 & 0 & 1 \end{bmatrix}$	$\begin{bmatrix} 0 \\ 0 \\ 0 \\ 0 \\ 0 \\ 0 \end{bmatrix}$	0
2	CFE_1	$\begin{bmatrix} 1 & 0 & 0 & 0 & 0.02 & 0 \\ 0 & 1 & 0 & -0.02 & 0 & 0 \\ 0 & 0 & 1 & 0 & 0 & 0 \\ 0 & 0 & 0 & 1 & 0 & 0 \\ 0 & 0 & 0 & 0 & 1 & 0 \\ 0 & 0 & 0 & 0 & 0 & 1 \end{bmatrix}$	$\begin{bmatrix} 0 \\ 0 \\ w_1 \\ \alpha_1 \\ \beta_1 \\ 0 \end{bmatrix}$	$-0.020/2 \le w_1 \le 0.020/2$ $-0.015/405 \le \alpha_1 \le 0.015/405$ $-0.015/405 \le \beta_1 \le 0.015/405$
3	IFE_2	$\begin{bmatrix} 1 & 0 & 0 & 0 & 450 & 0 \\ 0 & 1 & 0 & -450 & 0 & 0 \\ 0 & 0 & 1 & 0 & 0 & 0 \\ 0 & 0 & 0 & 1 & 0 & 0 \\ 0 & 0 & 0 & 0 & 1 & 0 \\ 0 & 0 & 0 & 0 & 0 & 1 \end{bmatrix}$	$\begin{bmatrix} 0 \\ 0 \\ 0 \\ 0 \\ 0 \\ 0 \end{bmatrix}$	0
4	CFE_2	$\begin{bmatrix} 1 & 0 & 0 & 0 & 0.02 & 0 \\ 0 & 1 & 0 & -0.02 & 0 & 0 \\ 0 & 0 & 1 & 0 & 0 & 0 \\ 0 & 0 & 0 & 1 & 0 & 0 \\ 0 & 0 & 0 & 0 & 1 & 0 \\ 0 & 0 & 0 & 0 & 0 & 1 \end{bmatrix}$	$\begin{bmatrix} 0 \\ 0 \\ w_2 \\ \alpha_2 \\ \beta_2 \\ 0 \end{bmatrix}$	$-0.020/2 \le w_2 \le 0.020/2$ $-0.015/410 \le \alpha_2 \le 0.015/410$ $-0.015/410 \le \beta_2 \le 0.015/410$
5	IFE_3	$\begin{bmatrix} 1 & 0 & 0 & 0 & 615 & 0 \\ 0 & 1 & 0 & -615 & 0 & 0 \\ 0 & 0 & 1 & 0 & 0 & 0 \\ 0 & 0 & 0 & 1 & 0 & 0 \\ 0 & 0 & 0 & 0 & 1 & 0 \\ 0 & 0 & 0 & 0 & 0 & 1 \end{bmatrix}$	$\begin{bmatrix} 0 \\ 0 \\ 0 \\ 0 \\ 0 \\ 0 \end{bmatrix}$	0
6	CFE_3	$\begin{bmatrix} 1 & 0 & 0 & 0 & 0.02 & 0 \\ 0 & 1 & 0 & -0.02 & 0 & 0 \\ 0 & 0 & 1 & 0 & 0 & 0 \\ 0 & 0 & 0 & 1 & 0 & 0 \\ 0 & 0 & 0 & 0 & 1 & 0 \\ 0 & 0 & 0 & 0 & 0 & 1 \end{bmatrix}$	$\begin{bmatrix} 0 \\ 0 \\ w_3 \\ \alpha_3 \\ \beta_3 \\ 0 \end{bmatrix}$	$-0.020/2 \le w_3 \le 0.020/2$ $-0.015/400 \le \alpha_3 \le 0.015/400$ $-0.015/400 \le \beta_3 \le 0.015/400$
7	IFE_4	$\begin{bmatrix} 1 & 0 & 0 & 0 & 980 & 0 \\ 0 & 1 & 0 & -980 & 0 & 0 \\ 0 & 0 & 1 & 0 & 0 & 0 \\ 0 & 0 & 0 & 1 & 0 & 0 \\ 0 & 0 & 0 & 0 & 1 & 0 \\ 0 & 0 & 0 & 0 & 0 & 1 \end{bmatrix}$	$\begin{bmatrix} 0 \\ 0 \\ 0 \\ 0 \\ 0 \\ 0 \end{bmatrix}$	0

Table 6 Distribution type and parameters of the FEs

No	Distribution pattern	Distribution parameter			
		β_1	β_2	β_3	β_4
1	Normal	$\mu = 0, \sigma = \frac{0.005}{405}$	$\mu = 0, \sigma = \frac{0.005}{410}$	$\mu = 0, \sigma = \frac{0.005}{400}$	$\mu = 0, \sigma = \frac{0.005}{440}$
2	Beta (right-skewed)	$\alpha = 2, \beta = 5$	$\alpha = 3, \beta = 4$	$\alpha = 2, \beta = 8$	$\alpha = 1.5, \beta = 3.2$
3	Beta (left-skewed)	$\alpha = 5, \beta = 2$	$\alpha = 4, \beta = 3$	$\alpha = 8, \beta = 2$	$\alpha = 3.2, \beta = 1.5$
4	Mixing	$\mu = 0, \sigma = \frac{0.005}{405}$ (Normal)	$\alpha = 5, \beta = 2$ (Beta)	$\alpha = 2, \beta = 5$ (Beta)	$a = -0.015/440$, $b = 0.015/440$ (Uniform)

Table 7 Distribution type and parameters of the FR

Parameter	Combination 1	Combination 2	Combination 3	Combination 4
Mean	0	0.0604	0.1396	0.0457
Variance	0.0125	0.0189	0.0189	0.0115
Skewness	0	0.3734	-0.3734	0.2417
Kurtosis	3	2.8210	2.8210	2.9311
Distribution pattern	IV	VI	VI	VI

Table 8 Qualification rate of four combinations

Method	Combination 1 (%)	Combination 2 (%)	Combination 3 (%)	Combination 4 (%)
Proposed method	99.88%	11.59%	0.00%	26.28%
MC method	99.84%	11.55%	0.00%	26.26%

5 Comparison and Discussion

5.1 Statistical Probability Analysis

Figure 7 has illustrated the variation distribution curve as well as MC statistical histograms according to Table 7. By comparing the results of the proposed method to Monte Carlo simulation, it was observed that the probability density curve agreed with the histogram statistics very well, as illustrated in Fig. 7a–d. Figure 7 also showed the qualification rate of the four combinations. In combination with Table 8, the relative error of qualification rate generated by the Pearson distribution family and MC method was less than 0.5 percent off. It turned out that the suggested method had a similar accuracy with MC method. In addition, the absolute time would be used as a measurement for comparison of the proposed method and MC simulation. The time function "tic & toc" was adopted in our MATLAB program to record the run time for the two methods. Table 9 has indicated the results.

As seen from the Table 9, the computation of the proposed method is almost instantaneous. Using an Intel Core (TM) 2, 1.83 GHz, 1.5 GB RAM computer, the average time consumption of this model is 0.025 s. But when performing traditional Monte Carlo simulation (the simulated number was set to 10,000 in this case), the average time consumption reaches up to 0.408 s, which is sixteen times of the proposed method. The result demonstrates that the Pearson distribution family method could enhance work efficiency significantly.

Additionally, as can be seen from Fig. 7, whenever the FE's variation distribution changed, the FR's distribution pattern and its corresponding probability form would bring about apparent changes. Similar changes have taken place in the results of the assembly qualified rate as well. To be specific, in the four groups of case results, normal distribution (combination 1) guaranteed the highest pass percentage of 99.8%, but the left-skewed distribution (combination 3) almost caused the qualified rate to be zero due to overlarge mean shift. In Fig. 7c, the mean shift reached up to 0.1396 mm, which directly led to most of the products to be unqualified.

All the above results demonstrated that part's variation distribution type had an important effect on the final assembly precision. The conventional hypothesis of normal distribution would not be able to describe the real variation conditions. And the Pearson distribution family method is an effective solution for complicated probability density function. Therefore, to predict the accurate assembly precision, each part's real variation distribution must be determined.

Fig. 7 Variation distribution curve and histogram: **a** combination 1, **b** combination 2, **c** combination 3, and **d** combination 4
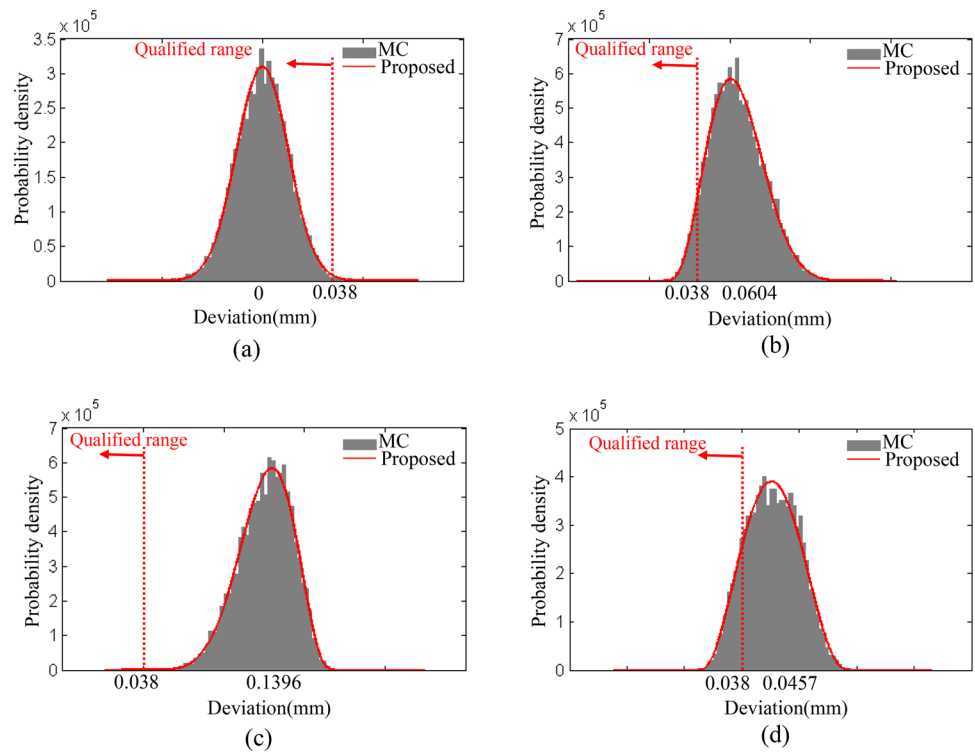

Table 9 Run time for the two methods

Method	Combination 1	Combination 2	Combination 3	Combination 4	Average
Proposed method	0.02 s	0.03 s	0.02 s	0.03 s	0.025 s
MC method	0.39 s	0.42 s	0.39 s	0.43 s	0.408 s

This required to take the practically assembling technology and the processing level into account during the phase of product design. Only this could make results be more reasonable and reliable.

It should be noted that in this paper the variation probability distribution of FE is regarded as a known condition. Historical manufacturing data of the parts should have been collected and analyzed firstly. So when we use a statistical variation analysis method to solve the distribution pattern of FR, the statistical variation results of FE can be directly invoked. However, MC simulation is an extremely time-consuming process, especially when a large number of data samples are desired to improve the FR's prediction accuracy. Apparently, the statistical variation of FR can be hardly achieved in time. This is an urgent problem to be solved in this paper.

5.2 Experimental Study

The experiment was carried out to verify the accuracy and reliability of the results presented in the case study. A
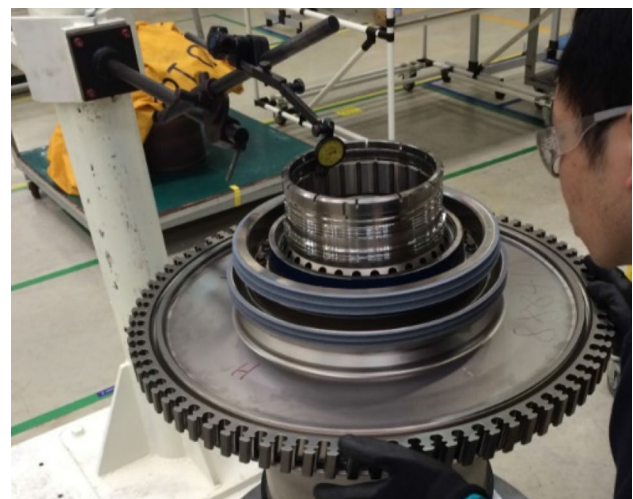

Fig. 8 Actual assembly process of HPTRs

group of high-pressure turbine rotors (HPTRs) of an aero-engine have been coupled on the same rotary main axis of the air-bearing turntable. Their structures, dimensions,

Table 10 Measured results

Item		Measured value	Predicted value
1	0.026		
2	0.025		
3	0.061		
4	0.048		
5	0.075	Mean 0.0452	Mean 0.0604
6	0.061	Variance 0.0186	Variance 0.0189
7	0.037		
8	0.077		
9	0.023		
10	0.057		
11	0.02		
12	0.043		
13	0.047		
14	0.042		
15	0.028		
16	0.069		
17	0.054		
18	0.066		
19	0.019		
20	0.026		
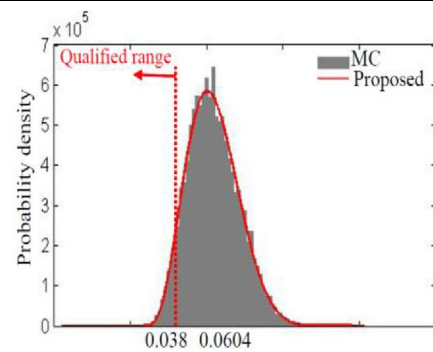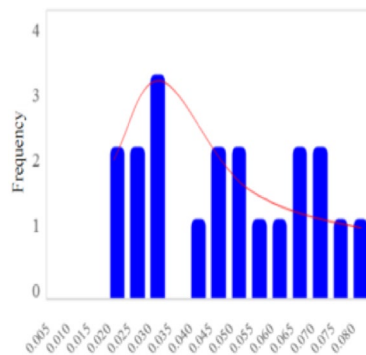
and tolerance specifications were the same as the case in Sect. 4. An axial dial indicator was used to measure the run-out value of the end face, and a radial dial indicator was used to measure the run-out value of the final component flange. The former was adopted to control tilt amount, and the latter was applied to characterize the concentricity. As shown in Fig. 8, the HPTRs were assembled randomly by top stage control: after one stage rotor installation, its concentricity was measured. If the concentricity was unqualified, the rotor part would be dismantled and rotated to a new installation angle, ensuring that the threshold condition of concentricity can be met after each part stacking. Then the next stage rotor was assembled upward.

Following this procedure, experiments have been implemented. Twenty times for repetitive assembly were completed. Measured data sets of the eccentricity of the top stage rotor were [0.026 0.025 0.061 0.048 0.075 0.061 0.037 0.077 0.023 0.057 0.020 0.043 0.047 0.042 0.028 0.069 0.054 0.066 0.019 0.026], the unit of which was millimetre, as shown in Table 10.

These statistics showed that the mean value of the repeated measures was 0.0452 mm, and the variance was 0.0186 mm², which was closer to the simulating result of combination 2 referred to the Table 7. The measured data

sets were further divided into several groups from 0.005 to 0.080 mm with interval step length 0.005 mm, and the variation distribution has been illustrated in Table 9. It was observed that the concentricity variation of the top stage rotor presented a typical right-skewed distribution, which conformed to the prediction results of combination 2 that was shown in Fig. 7b. These results proved that measured data in a certain error range accorded well with the calculations. The variation analysis method suggested in this paper was conducive to precision prediction and tolerance design for revolving components assembly.

6 Conclusions

This work was attempting to propose a novel variation analysis method for revolving components assembly. A calculating scheme was illustrated on a realistic case originating in aero-engine subassembly. Following conclusions could be drawn:

(1) Unified Jacobian–Torsor theory was used to establish the serial kinematic chain, which combined the advantages of the torsor model which was suitable for

variation representation and the Jacobian matrix which was suitable for variation propagation. For aero-engine rotors which contain lots of geometric variations and composite features, Jacobian–Torsor theory can effectively solve the 3D variation modelling.

(2) Pearson distribution family method was used to perform statistical variation analysis. Compared to MC results with 10,000 simulation times consuming 0.408 s, this novel method has a similar accuracy, but much higher efficiency (the average time consumption is 0.025 s).

(3) The result of FR depends on each FE's probability distribution pattern significantly. To obtain more accurate predictions, the real distribution states of parts variations should be detected and used, which is beneficial to tolerance design and performance forecast.

References

1. Hu J, Zhang K, Cheng H et al (2020) An experimental investigation on interfacial behavior and preload response of composite bolted interference-fit joints under assembly and thermal conditions. Aerosp Sci Technol 103:105917
2. Zhang HX, Li XJ, Jiang L et al (2019) A review of misalignment of aero-engine rotor system. Acta Aeronaut Astronaut Sin 40(6):022717
3. Forouraghi B (2002) Worst-Case Tolerance design and quality assurance via genetic algorithms. J Optim Theory Appl 113:251–268
4. Dantan JY, Qureshi AJ (2009) Worst-case and statistical tolerance analysis based on quantified constraint satisfaction problems and Monte Carlo simulation. Comput Aided Des 41:1–12
5. Gordon R, Pickering M, Bisson D (1984) Uncertainty analysis by the "worst case" method. J Chem Educ 61:780
6. Fei C, Bai G (2012) Extremum selection method of random variable for nonlinear dynamic reliability analysis of turbine blade deformation. Propuls Power Res 1:58–63
7. Lin CY, Huang WH, Jeng MC, Doong JL (1997) Study of an assembly tolerance allocation model based on Monte Carlo simulation. J Mater Process Technol 70:9–16
8. Knutson K, Schexnayder C, Fente J (2005) Describing a beta probability distribution function for construction simulation. J Constr Eng Manag 131:221–229
9. Nigam SD, Turner JU (1995) Review of statistical approaches to tolerance analysis. Comput Aided Des 27:6–15
10. Yun W, Lu Z, He P et al (2020) Parameter global reliability sensitivity analysis with meta-models: a probability estimation-driven approach. Aerosp Sci Technol 106:106040
11. Han L, Chen C, Guo T et al (2021) Probability-based service safety life prediction approach of raw and treated turbine blades regarding combined cycle fatigue. Aerosp Sci Technol 110:106513
12. Lin EE, Zhang HC (2001) Theoretical tolerance stackup analysis based on tolerance zone analysis. Int J Adv Manuf Technol 17:257–262
13. Wu F, Dantan JY, Etienne A, Siadat A, Martin P (2009) Improved algorithm for tolerance allocation based on Monte Carlo simulation and discrete optimization. Comput Ind Eng 56:1402–1413
14. Toft N, Innocent GT, Gettinby G, Reid SW (2007) Assessing the convergence of Markov Chain Monte Carlo methods: an example from evaluation of diagnostic tests in absence of a gold standard. Prev Vet Med 79:244–256
15. Gong C, Ma BF (2019) Shape optimization and sensitivity analysis of a morphing-wing aircraft. Int J Aeronaut Space Sci 20:57–69
16. Ata MY (2007) A convergence criterion for the Monte Carlo estimates. Simul Model Pract Theory 15:237–246
17. Lin F, Chen C, Chen J et al (2020) Dimensional synthesis of antenna-deployable support structure. Int J Aeronaut Space Sci 21:404–417
18. Liu Y, Zhang M, Sun C et al (2019) A method to minimize stage-by-stage initial unbalance in the aero engine assembly of multi-stage rotors. Aerosp Sci Technol 85:270–276
19. Roy U, Li B (1999) Representation and interpretation of geometric tolerances for polyhedral objects. II.: size, orientation and position tolerances. Comput Aided Des 31:273–285
20. Cai M, Yang JX, Wu ZT (2004) Mathematical model of cylindrical form tolerance. J Zhejiang Univ Sci 5:890–895
21. Roy U, Liu CR, Woo TC (1991) Review of dimensioning and tolerancing: representation and processing. Comput Aided Des 23:466–483
22. Chen KZ, Feng XA, Lu QS (2002) Intelligent location-dimensioning of cylindrical surfaces in mechanical parts. Comput Aided Des 34:185–194
23. Whitney DE, Gilbert OL (1994) Representation of geometric variations using matrix transforms for statistical tolerance analysis in assemblies. In: IEEE international conference on robotics and automation, 1993 proceedings, vol 1994(2), pp 314–321
24. Fei CW, Li H, Liu HT et al (2020) Multilevel nested reliability-based design optimization with hybrid intelligent regression for operating assembly relationship. Aerosp Sci Technol 103:105906
25. Jayaweera N, Webb P, Johnson C (2010) Measurement assisted robotic assembly of fabricated aero-engine components. Assem Autom 30(10):56–65
26. Yang Z, Mcwilliam S, Popov AA, Hussain T (2013) A probabilistic approach to variation propagation control for straight build in mechanical assembly. Int J Adv Manuf Technol 64:1029–1047
27. Ghie W (2016) Statistical analysis tolerance using jacobian torsor model based on uncertainty propagation method. Int J Multiphys 3:11–30

28. Ahsanullah M, Hamedani GG (2012) Characterizations of certain continuous univariate distributions based on the conditional distribution of generalized order statistics. Pak J Stat 28:253–258

29. Kharoufeh JP, Chandra MJ (2002) Statistical tolerance analysis for non-normal or correlated normal component characteristics. Int J Prod Res 40:337–352

30. Provost SB (2016) A brief derivation of the asymptotic distribution of Pearson's statistic and an accurate approximation to its exact distribution. In: Li W, Stanford D, Yu H (eds) Advances in time series methods and applications. Fields institute communications, vol 78. Springer, New York, NY. https://doi.org/10.1007/978-1-4939-6568-7_11

31. Nagahara Y (2004) A method of simulating multivariate nonnormal distributions by the Pearson distribution system and estimation. Comput Stat Data Anal 47:1–29

32. Gao J, Chase KW, Magleby SP (1998) General 3-D tolerance analysis of mechanical assemblies with small kinematic adjustments. Iie Trans 30:367–377

33. Chase KW, Gao J, Magleby SP, Sorensen CD (1996) Including geometric feature variations in tolerance analysis of mechanical assembly. IIE Trans 28(10):795–807

34. Davidson JK, Mujezinović A, Shah JJ (2002) A new mathematical model for geometric tolerances as applied to round faces. ASME J Mech Des 124:609–622

35. Davidson JK, Shah JJ, Mujezinovié A (2005) Method and apparatus for geometric variations to integrate parametric computer-aided design with tolerance analysis and optimization. US Patent 6963824

36. Desrochers A, Rivière A (1997) A matrix approach to the representation of tolerance zones and clearances. Int J Adv Manuf Technol 13:630–636

37. Whitney DE, Gilbert OL, Jastrzebski M (1994) Representation of geometric variations using matrix transforms for statistical tolerance analysis in assemblies. Res Eng Des 6(4):191–210

38. Desrochers A, Ghie W, Laperrière L (2003) Application of a unified Jacobian–Torsor model for tolerance analysis. J Comput Inf Sci Eng 3:2–14

39. Laperrière L, Ghie W, Desrochers A (2002) Statistical and deterministic tolerance analysis and synthesis using a unified Jacobian–Torsor model. CIRP Ann Manuf Technol 51:417–420

40. Hervé JM (1978) Analyse structurelle des mécanismes par groupe des déplacements. Mech Mach Theory 13:437–450

41. Laperrière L, Desrochers A (2001) Modeling assembly quality requirements using Jacobian or screw transforms: a comparison. In: Assembly and task planning, proceedings of the IEEE international symposium on, pp 330–336

42. Marziale M, Polini W (2011) A review of two models for tolerance analysis of an assembly: Jacobian and Torsor. Int J Comput Integr Manuf 24(1):74–86

43. Karpov IG, Zyryanov YT (2015) On modified Pearson distributions and their identification. Autom Control Comput Sci 49:366–372

44. Solvang HK, Nagahara Y, Araki S, Sawada H, Makino S (2009) Frequency-domain Pearson distribution approach for independent component analysis (FD-Pearson-ICA) in blind source separation. IEEE Trans Audio Speech Lang Process 17:639–649

45. Trenkler G (1994) Continuous univariate distributions In: Johnson, NL, Kotz, S, Balakrishnan, N (eds) vol 1, 2nd edn. Wiley, New York, pp 756

46. Leitch M (2015) 3. Some types of probability distribution. Wiley